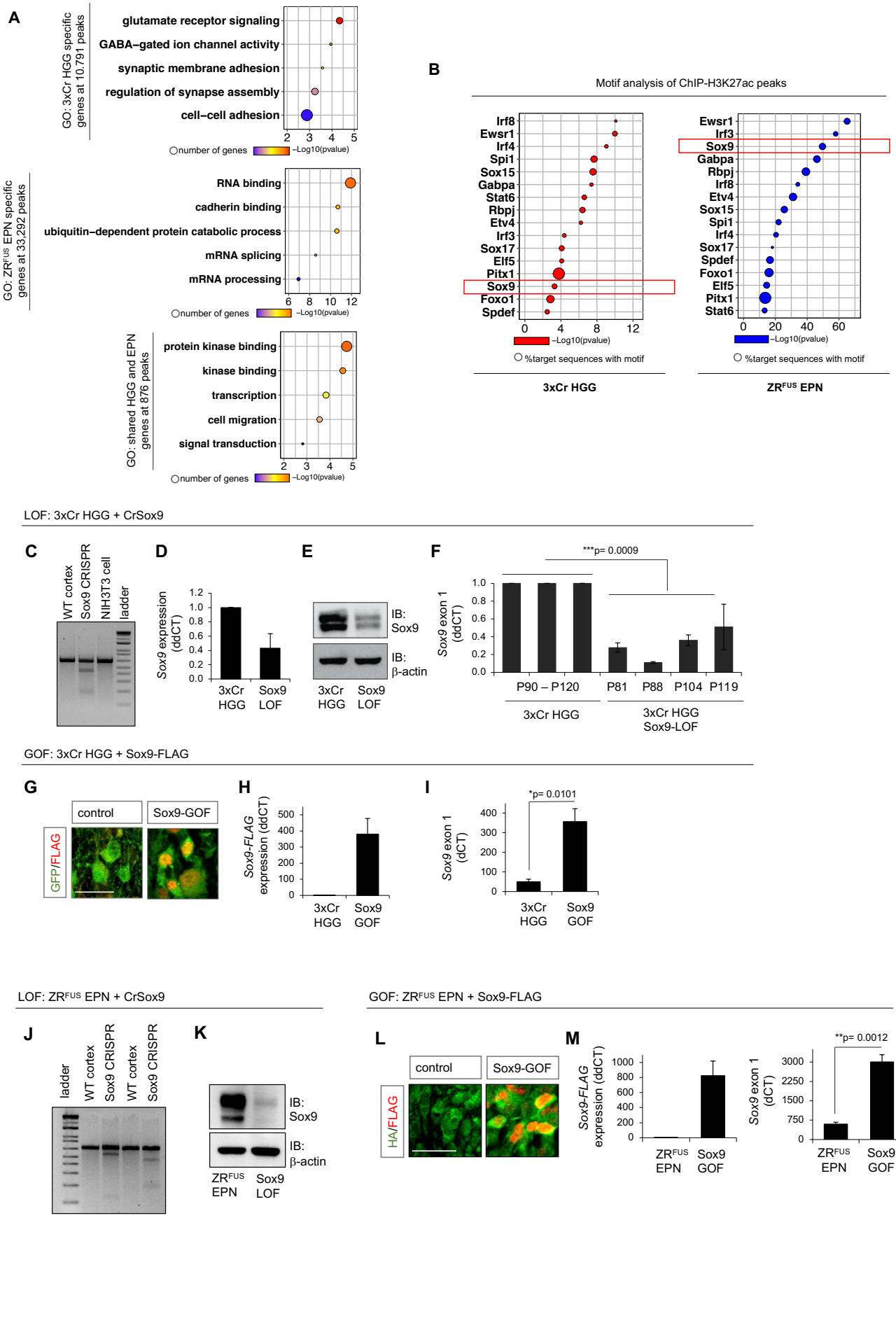
A
GO: 3xCr HGG specific genes at 10.791 peaks
glutamate receptor signaling
GABA–gated ion channel activity
synaptic membrane adhesion
regulation of synapse assembly
cell–cell adhesion
number of genes
–Log10(pvalue)
GO: ZRFUS EPN specific genes at 33,292 peaks
RNA binding
cadherin binding
ubiquitin–dependent protein catabolic process
mRNA splicing
mRNA processing
GO: shared HGG and EPN genes at 876 peaks
protein kinase binding
kinase binding
transcription
cell migration
signal transduction
B
Motif analysis of ChIP-H3K27ac peaks
Irf8
Ewsr1
Irf4
Spi1
Sox15
Gabpa
Stat6
Rbpj
Etv4
Irf3
Sox17
Elf5
Pitx1
Sox9
Foxo1
Spdef
%target sequences with motif
3xCr HGG
ZRFUS EPN
LOF: 3xCr HGG + CrSox9
C
WT cortex
Sox9 CRISPR
NIH3T3 cell
ladder
D
Sox9 expression (ddCT)
3xCr HGG
Sox9 LOF
E
IB: Sox9
IB: β-actin
F
***p= 0.0009
Sox9 exon 1 (ddCT)
P90 – P120
P81
P88
P104
P119
3xCr HGG
3xCr HGG Sox9-LOF
GOF: 3xCr HGG + Sox9-FLAG
G
control
Sox9-GOF
GFP/FLAG
H
Sox9-FLAG expression (ddCT)
Sox9 GOF
I
*p= 0.0101
Sox9 exon 1 (dCT)
LOF: ZRFUS EPN + CrSox9
J
ladder
K
ZRFUS EPN
GOF: ZRFUS EPN + Sox9-FLAG
L
HA/FLAG
M
**p= 0.0012

Supporting Figure 1. Epigenetic states of H3K27ac 3xCr HGG and ZR^{FUS} EPN tumors subtypes and effect of Sox9 manipulation on these tumors.

(A) GO analysis of genes carrying H3K27ac peaks that are unique to 3xCr HGG, ZR^{FUS} EPN or shared between both. (B) Analysis of transcription factor motif enrichment at 1000 bp from H3K27ac peak center revealed association with 16 transcription factors in both 3xCr HGG and ZR^{FUS} EPN. (C) Surveyor Nuclease Digestion assay of *Sox9* gRNA efficiency in LOF HGG tumor using NIH-3T3 cells as negative control. (D) RT-qPCR fold-enrichment (ddCT) of *Sox9* transcript in control and LOF HGG tumors after normalization using *Gapdh* (n=3 mice per group). Data shown as mean ± s.e.m. (E) Western blot of Sox9 and Gapdh loading control in HGG control and LOF HGG whole cell lysates. (F) RT-qPCR fold-enrichment (ddCT) of *Sox9* in control and LOF HGG tumors across a series of time-points, after normalization using *Gapdh*. Primers were designed to span exon 1, which was targeted by the CRISPR/Cas9 gRNA used for Sox9 deletion. Data shown as mean ± s.e.m. Two-tailed Student's t-test. (G) IF staining of FLAG colabeling with GFP in control and GOF HGG tumors showing no FLAG signal in 3xCr HGG control; scale bar: 25 μm. (H) RT-qPCR fold-enrichment (ddCT) of *Sox9* transcript in control and GOF HGG tumors, after normalization using *Gapdh* (n=3 mice per group). Data shown as mean ± s.e.m. (I) RT-qPCR fold-enrichment (dCT) of *Sox9* exon1 in control and GOF HGG tumors, after normalization using *Gapdh*. Data shown as mean ± s.e.m. Two-tailed Student's t-test. (J) Surveyor Nuclease Digestion assay of *Sox9* gRNA efficiency in LOF EPN tumor. From left to right, lanes 2-3 and lanes 4-5 represent reactions using different primer sets to detect mismatch. (K) Western blot of Sox9 and b-actin loading control in control and LOF EPN whole cell lysates. (L) IF staining of FLAG colabeling with HA tag (fused to ZR^{FUS}) in control and GOF EPN tumors showing no FLAG signal in EPN control; scale bar: 50 μm. (M) RT-qPCR fold-enrichment (ddCT) of *Sox9* transcript in control and GOF EPN tumors, after normalization using *Gapdh* (n=3 mice per group). Data shown as mean ± s.e.m. RT-qPCR fold-enrichment (dCT) of *Sox9* exon1 in control and GOF EPN tumors, after normalization using *Gapdh*. Data shown as mean ± s.e.m. Two-tailed Student's t-test.

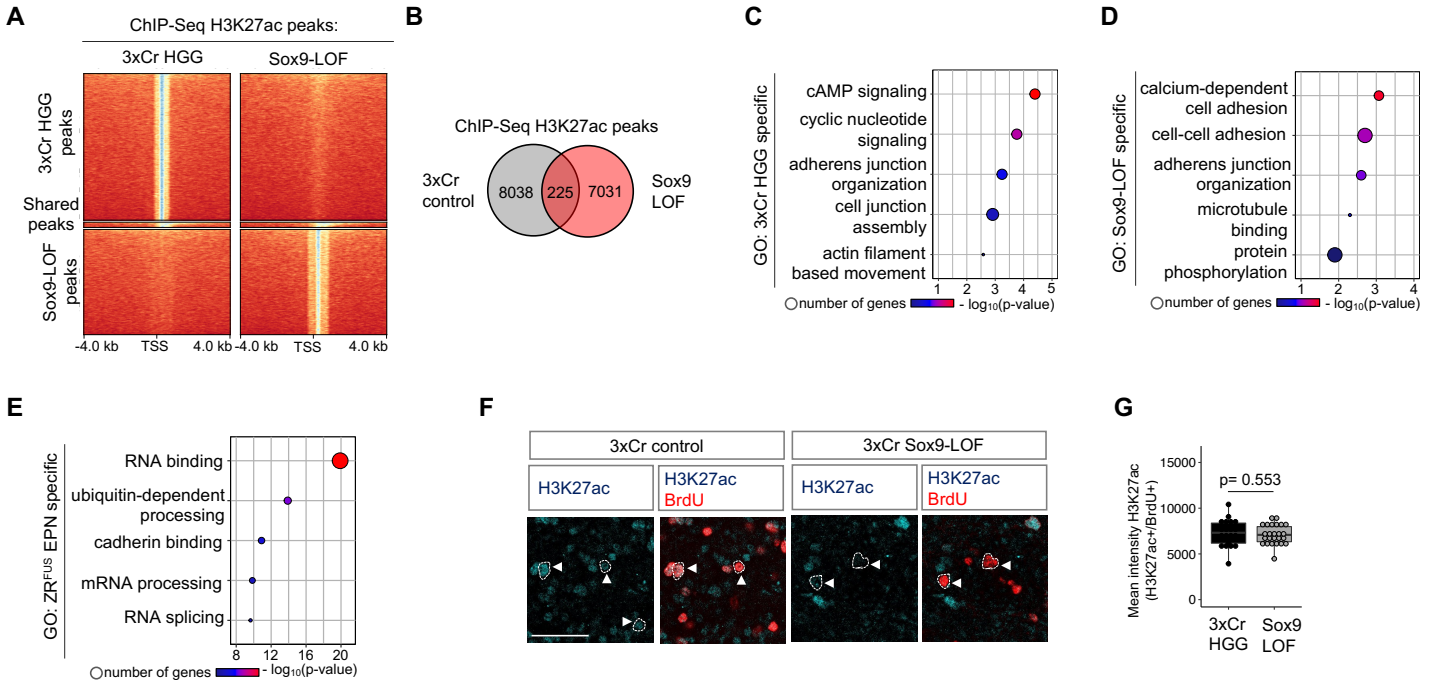

Supporting Figure 2. Sox9 differentially regulates H3K27ac states in 3xCr HGG and ZR^{FUS} EPN tumors subtypes.

(A) Comparison showing heatmaps of ChIP-H3K27ac signal at 4 kb from peak center in control versus Sox9-LOF HGG. (B) Venn diagram of number peaks unique to control, Sox9-LOF HGG and overlapping across two independent biological replicates. (C-D) GO analysis of genes carrying H3K27ac peaks unique to control and Sox9-LOF HGG, and (E) unique to EPN control in comparison to Sox9-GOF EPN. (F) Representative images of H3K27ac colabeled with BrdU staining in P90 control and Sox9-LOF HGG tumors and (H) box plots showing quantification of H3K27ac fluorescence intensity in BrdU positive cells (n=3 mice per group, 20-30 cells each; scale bar: 50 μm). *P*-values calculated using one-way ANOVA with Tukey's test.

A

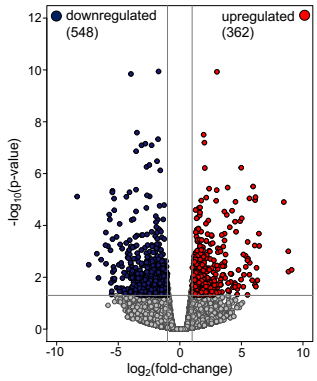

3xCr HGG: Sox9-LOF vs 3xCr control

B

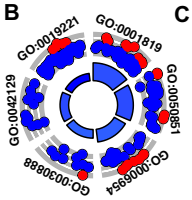

C

GO ID	GO Term associated with:	p-value
GO:0001819	cytokine production	7.94E-08
GO:0050851	antigen receptor-mediated signaling pathway	3.21E-07
GO:0006954	inflammatory response	2.21E-06
GO:0030888	B-cell proliferation	3.34E-05
GO:0042129	T-cell proliferation	3.55E-05
GO:0019221	cytokine mediated signaling	7.13E-05

D

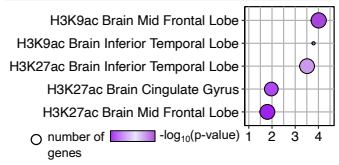

3xCr HGG: Sox9-GOF vs 3xCr control

F

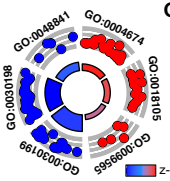

G

GO ID	GO Term associated with:	p-value
GO:0004674	protein kinase activity	2.20E-04
GO:0018105	peptidyl phosphorylation	3.89E-04
GO:0099565	chemical synaptic transmission	9.20E-04
GO:0030199	collagen fibril organization	1.71E-08
GO:0030198	extracellular matrix organization	6.45E-08
GO:0048841	axon guidance	3.56E-05

E

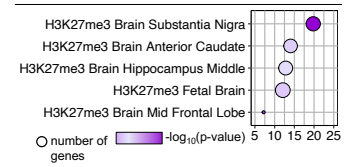

ZRFUS EPN: Sox9-GOF vs ZRFUS control

H

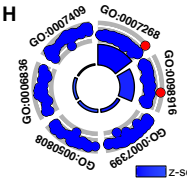

I

GO ID	GO Term associated with:	p-value
GO:0007268	synaptic transmission	9.30E-44
GO:0098916	trans-synaptic signaling	1.33E-35
GO:0007399	nervous system development	6.32E-21
GO:0050808	synapse organization	8.19E-21
GO:0006836	neurotransmitter transport	2.21E-20
GO:0007409	axonogenesis	1.62E-18

J

K

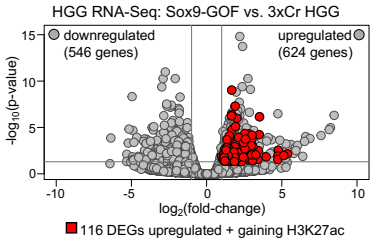

L

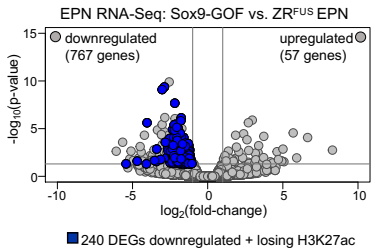

Supporting Figure 3. Sox9 differentially regulates gene expression in 3xCr HGG and ZR^{FUS} EPN tumors subtypes.

(A) Volcano plots depicting RNA-Seq data comparing 3xCr control versus Sox9-LOF HGG. RNA-Seq experiments were performed in independent biological triplicates ($P < 0.05$ and fold-change > 2). (B) Gene ontology circle plot and table of associated GO terms in DEGs of Sox9-LOF versus HGG control. (C) Grid plots showing DEGs in Sox9-GOF in (D) 3xCr HGG and (E) ZR^{FUS} EPN associated with histone marks in central nervous system tissues. Data derived from Epigenomic Roadmap using Enrichr. (F-G) Gene ontology circle plot and table of associated GO terms in DEGs of Sox9-GOF versus HGG control. (H-I) Gene ontology circle plot and table of associated GO terms in DEGs of Sox9-GOF versus EPN control. (J) Relative transcript expression of lineage markers obtained from RNA-Seq data of HGG Sox9-GOF vs. control 3xCr HGG and EPN Sox9-GOF vs ZR^{FUS} EPN. (K-L) Volcano plots depicting the 116 upregulated DEGs and 240 downregulated DEGs in 3xCr HGG and ZR^{FUS} EPN, identified in Fig. 3E.

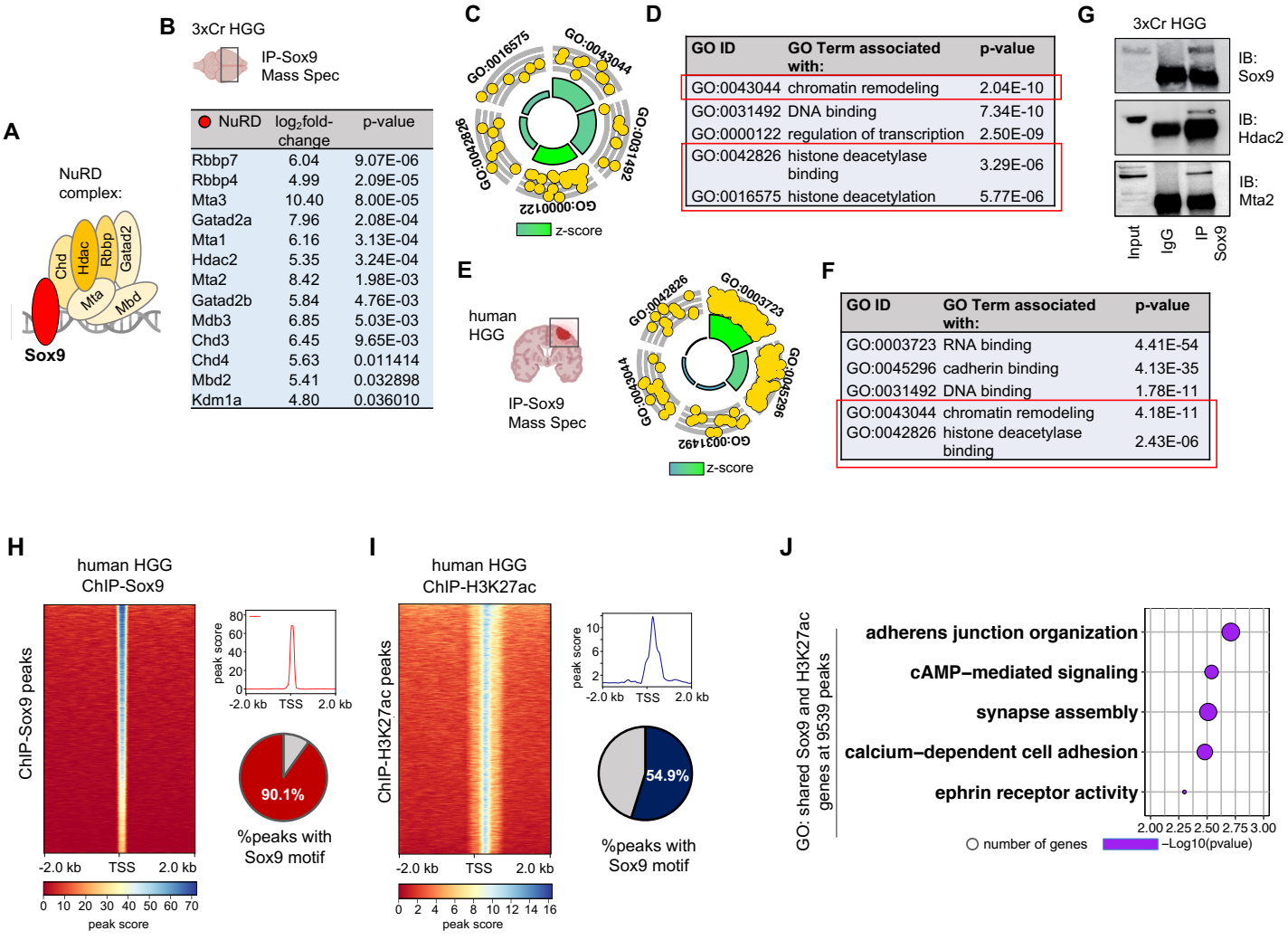

NuRD	log_2fold-change	p-value
Rbbp7	6.04	9.07E-06
Rbbp4	4.99	2.09E-05
Mta3	10.40	8.00E-05
Gatad2a	7.96	2.08E-04
Mta1	6.16	3.13E-04
Hdac2	5.35	3.24E-04
Mta2	8.42	1.98E-03
Gatad2b	5.84	4.76E-03
Mdb3	6.85	5.03E-03
Chd3	6.45	9.65E-03
Chd4	5.63	0.011414
Mbd2	5.41	0.032898
Kdm1a	4.80	0.036010

GO ID	GO Term associated with:	p-value
GO:0043044	chromatin remodeling	2.04E-10
GO:0031492	DNA binding	7.34E-10
GO:0000122	regulation of transcription	2.50E-09
GO:0042826	histone deacetylase binding	3.29E-06
GO:0016575	histone deacetylation	5.77E-06

GO ID	GO Term associated with:	p-value
GO:0003723	RNA binding	4.41E-54
GO:0045296	cadherin binding	4.13E-35
GO:0031492	DNA binding	1.78E-11
GO:0043044	chromatin remodeling	4.18E-11
GO:0042826	histone deacetylase binding	2.43E-06

Supporting Figure 4. Sox9 interacts with histone deacetylation complex in HGG.

(A) Schematic of NuRD members and (B) table showing Sox9 binding fold-change and *P*-values with NuRD complex members from 3xCr HGG IP-MS data. (C-F) Gene ontology circle plot and table of associated GO terms of proteins from Sox9 interactome in (C-D) 3xCr HGG and (E-F) human HGG. (G) Sox9 co-immunoprecipitation experiments with NuRD members Hdac2 and Mta2 from 3xCr HGG nuclear lysates. (H-I) Heatmaps and Sox9 motif analysis of (H) ChIP-Sox9 and (I) ChIP-H3K27ac signal at 2 kb from peak center in human HGG. Sox9 motif analysis was done at 1000 bp from peak center. (J) GO terms associated with H3K27ac and Sox9 co-occupied peaks shown in Fig. 4I.

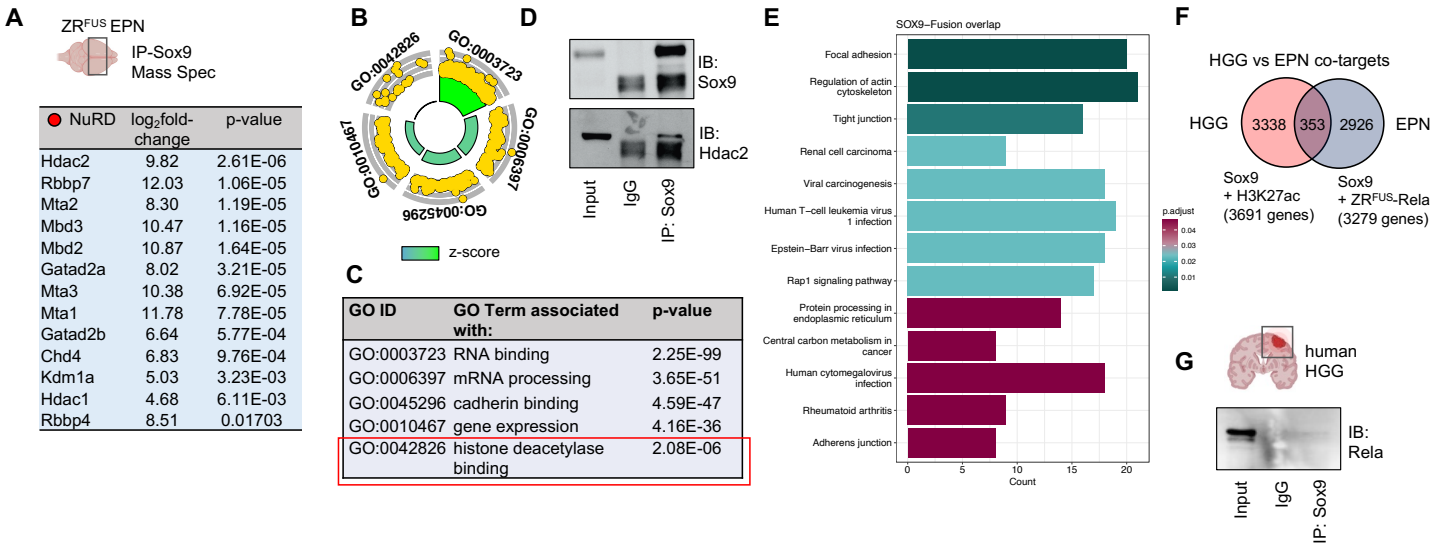

C

GO ID	GO Term associated with:	p-value
GO:0003723	RNA binding	2.25E-99
GO:0006397	mRNA processing	3.65E-51
GO:0045296	cadherin binding	4.59E-47
GO:0010467	gene expression	4.16E-36
GO:0042826	histone deacetylase binding	2.08E-06

A

NuRD	log_2fold-change	p-value
Hdac2	9.82	2.61E-06
Rbbp7	12.03	1.06E-05
Mta2	8.30	1.19E-05
Mbd3	10.47	1.16E-05
Mbd2	10.87	1.64E-05
Gatad2a	8.02	3.21E-05
Mta3	10.38	6.92E-05
Mta1	11.78	7.78E-05
Gatad2b	6.64	5.77E-04
Chd4	6.83	9.76E-04
Kdm1a	5.03	3.23E-03
Hdac1	4.68	6.11E-03
Rbbp4	8.51	0.01703

Supporting Figure 5. Sox9 interacts with ZFTA-Rela and co-regulates oncogenic programs in ZR^{FUS} EPN.

(A) Table showing Sox9 binding fold-change and *P*-values with NuRD complex members from ZR^{FUS} EPN IP-MS data. (B-C) Gene ontology circle plot and table of associated GO terms of proteins from Sox9 interactome in ZR^{FUS} EPN. (D) Sox9 co-immunoprecipitation experiments with NuRD member Hdac2 from ZR^{FUS} EPN lysates. (E) KEGG pathway terms associated with Sox9 and ZFTA-Rela fusion co-targets. (F) Venn diagram of genes shared between of Sox9-H3K27ac co-targets in HGG with Sox9-ZR$^{FUS.}$ co-targets in EPN. (G) Sox9 co-immunoprecipitation with Rela from human HGG nuclear lysate.

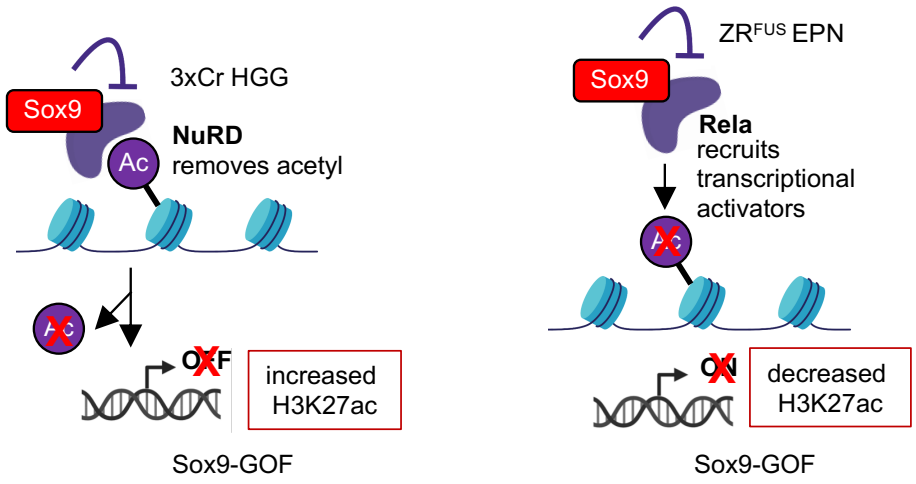

Supporting Figure 6. Model of differential Sox9 control on H3K27ac epigenetic states in HGG and EPN.